HHS Public Access

Author manuscript

J Am Coll Cardiol. Author manuscript; available in PMC 2017 December 06.

Published in final edited form as:

J Am Coll Cardiol. 2016 December 06; 68(22): 2454–2464. doi:10.1016/j.jacc.2016.09.925.

Pim1 Kinase Overexpression Enhances Ckit+ Cardiac Stem Cell Cardiac Repair Following Myocardial Infarction in Swine

Shathiyah Kulandavelu, PhD[a], **Vasileios Karantalis, MD**[a], **Julia Fritsch, BS**[a], **Konstantinos E. Hatzistergos, PhD**[a], **Viky Y. Loescher, MD**[a], **Frederic McCall, BS**[a], **Bo Wang, MD**[a], **Luiza Bagno, PhD**[a], **Samuel Golpanian, MD**[a], **Ariel Wolf, BS**[a], **Justin Grenet, BS**[a], **Adam Williams, MD**[a], **Aaron Kupin**[a], **Aaron Rosenfeld**[a], **Sadia Mohsin, PhD**[b], **Mark A. Sussman, PhD**[b], **Azorides Morales, MD**[c], **Wayne Balkan, PhD**[a,c], and **Joshua M. Hare, MD**[a,c]

[a]The Interdisciplinary Stem Cell Institute, University of Miami, Miller School of Medicine, Miami, Florida

[b]Biology Department and Integrated Regenerative Research Institute, San Diego State University, San Diego, California

[c]Department of Medicine, University of Miami, Miller School of Medicine, Miami, Florida

Abstract

BACKGROUND—Pim1 kinase plays an important role in cell division, survival, and commitment of precursor cells towards a myocardial lineage, and overexpression of Pim1 in ckit+ cardiac stem cell (CSC) enhances their cardioreparative properties.

OBJECTIVES—We sought to validate the effect of Pim1-modified CSCs in a translationally relevant large animal preclinical model of myocardial infarction (MI).

METHODS—Human CSCs (hCSCs, n = 10), hckit+ CSCs overexpressing Pim1 (Pim1+; n = 9), or placebo (n = 10) were delivered by intramyocardial injection to immunosuppressed Yorkshire swine (n = 29) 2 weeks after MI. Cardiac magnetic resonance and pressure volume loops were obtained before and after cell administration.

Corresponding Author: Joshua M. Hare, MD, Louis Lemberg Professor of Medicine, Director, Interdisciplinary Stem Cell Institute, University of Miami Miller School of Medicine, Biomedical Research Building, 1501 N.W. 10th Avenue, Room 824 P.O Box 016960 (R125), Miami, Florida 33101, Telephone: 305- 243-1999, Fax: 305-243-5584, jhare@med.miami.edu.
Drs. Kulandavelu and Karantalis contributed equally.

Disclosures: Dr. Kulandavelu – nothing to disclose; Dr. Karantalis – nothing to disclose; Julia Fritsch – nothing to disclose; Dr. Konstantinos E. Hatzistergos – Vestion Inc. that includes equity, member of the scientific advisory board and consulting. Vestion did not contribute funding to this study; Dr. Viky Y. Loescher – nothing to disclose; Frederic McCall – nothing to disclose; Dr. Bo Wang – nothing to disclose; Dr. Luiza L. Bagno – nothing to disclose; Dr. Samuel Golpanian – nothing to disclose; Ariel Wolf – nothing to disclose; Justin Grenet – nothing to disclose; Dr. Adam Williams – nothing to disclose; Aaron Kupin – nothing to disclose; Aaron Rosenfeld – nothing to disclose; Dr. Sadia Mohsin – nothing to disclose; Dr. Mark Sussman – co-founder of CardioCreate, Inc. CardioCreate did not contribute funding to this study; Dr. Azorides Morales –Sakura Finetek, USA patent royalties. Sakura Finetek, USA did not contribute funding to this study; Dr. Wayne Balkan – nothing to disclose; Dr. Joshua Hare – Vestion Inc. that includes equity, board membership and consulting. Vestion did not contribute funding to this study.

RESULTS—Whereas both hCSCs reduced MI size compared to placebo, Pim1$^+$ cells produced a ~3-fold greater decrease in scar mass at 8 weeks post-injection compared to hCSCs (−29.2 ± 2.7% vs. −8.4 ± 0.7%; $p < 0.003$). Pim1$^+$ hCSCs also produced a 2-fold increase of viable mass compared to hCSCs at 8 weeks (113.7 ± 7.2% vs. 65.6 ± 6.8%; $p < 0.003$), and a greater increase in regional contractility in both infarct and border zones (both $p < 0.05$). Both CSC types significantly increased ejection fraction at 4 weeks but this was only sustained in the Pim1$^+$ group at 8 weeks compared to placebo. Both hCSC and Pim1+ hCSC treatment reduced afterload ($p=0.02$ and $p=0.004$, respectively). Mechanoenergetic recoupling was significantly greater in the Pim1+ hCSC group ($p = 0.005$).

CONCLUSIONS—Pim1 overexpression enhanced the effect of intramyocardial delivery of CSCs to infarcted porcine hearts. These findings provide a rationale for genetic modification of stem cells and consequent translation to clinical trials.

Keywords

heart failure; human cardiac progenitor cells; injection; pressure volume

Stem cell therapy improves cardiac structure and function post-myocardial infarction (MI), but current approaches lead to only modest cell survival, proliferation, and cell commitment post-injection, which may contribute to limited therapeutic responses (1). Ex vivo genetic modification of stem cells bolsters therapeutic effects by increasing cell survival and secretion of paracrine factors, enhancing endogenous repair processes, and contributing to newly formed myocardium (2). Pim1 is a proto-oncogenic serine-threonine kinase that was originally discovered as the proviral integration site for Moloney murine leukemia virus (3). Injecting human ckit$^+$ cardiac stem cells (hCSCs) overexpressing Pim1 into infarcted mouse hearts produced enhanced cardioprotective effects based on greater cellular proliferation and attenuated apoptosis, as well as greater inhibition of hypertrophic signaling (4).

Part of a family of constitutively activated serine/threonine kinases, Pim1 works in concert with its downstream target, Akt kinase, to regulate cell survival and proliferation (5). While Pim1 expression is developmentally downregulated in the context of the myocardium as the heart ages (5), its expression is upregulated in cardiomyocytes after pressure overload or infarction challenge (3), suggesting that Pim1 serves an important protective role in the heart. Substrates associated with the antiapoptotic effects of Pim1 overexpression include increased Bcl-X_L and Bcl-2 protein levels and BAD phosphorylation (5). Mechanisms involved in the proliferative-promoting effects of Pim1 include increased phosphorylation of the cyclin-dependent kinase inhibitor p21 and stabilization of c-Myc and the nuclear mitotic apparatus (6). In the hearts of infarcted female mice, introduction of hCSCs modified with enhanced green fluorescent protein (egfp)+Pim1 (Pim1+ hCSC) produced increased hCSC proliferation, differentiation, cardiac function, neovascularization, de novo myocyte formation, scar reduction, and the number of ckit+ cells (2). However, given the limitations of translating murine findings into large mammals, including humans, we hypothesized that genetically modified hCSCs overexpressing Pim1 might possess enhanced cardioprotective ability compared to regular ckit+ CSCs in a swine model.

Methods

All animal protocols were reviewed and approved by the University of Miami Institutional Animal Use and Care Committee. Twenty-nine female Yorkshire swine underwent experimental MI (7). Animals were randomized and received direct transepicardial injections via mini thoracotomy of 1 of the following treatment groups: 1) 1 x 106 hCSCs; 2) 1 x 106 hCSCs modified to overexpress Pim1 (Pim1+ hCSC); or 3) placebo (Plasma-Lyte, Baxter Healthcare Corporation, Deerfield, Illinois). These doses were determined from our previous work using a xenogenic mouse model of heart disease (4). Each study animal underwent extensive evaluation for safety of the treatment. Additionally, noninvasive imaging using cardiac magnetic resonance (CMR) and invasive hemodynamic assessment was performed.

Experiments were conducted in Yorkshire female swine, a large animal model of infarction and reperfusion (7) ideal for translation of cardiovascular research to human application. Animals in this study underwent closed-chest ischemic reperfusion MI, in which infarction was induced by inflation of a coronary angioplasty balloon in the mid left anterior descending artery for 90 min as previously described (7). This study was composed of 2 branches of identical design but different length of follow-up (4 or 8 weeks post-injection).

A left mini-thoracotomy (8) was created with a small 4 to 5 cm incision in the fifth anterior/lateral intercostal space and the left plural cavity was entered under direct visualization. A 5 mm port was placed in the sixth or seventh intercostal space and a 5 mm endoscope (Karl Storz, Tuttlingen, Germany) was inserted into the left chest cavity. The pericardium was opened and the infarct area identified by wall motion abnormalities and correlation with coronary anatomy. A curved 27-gauge needle was inserted tangentially into the myocardium and 10 injections (0.5 ml each) administered into the infarct border zone. A 12-F chest tube was inserted into the left pleural cavity via the port incision and tunneled through the chest wall. All incisions were closed and the chest tube placed to -20 cm of underwater suction to evacuate the pneumothorax. Fluoroscopy confirmed lung expansion and the chest tube was removed before extubation. Animals were allowed to recover and provided postoperative analgesia.

Swine (cell- and placebo-treated) were placed on cyclosporine and methylprednisolone therapy to prevent rejection of human stem cell transplants. Twelve days post-MI, animals received cyclosporine 400 mg PO twice daily. Serum trough levels were measured at least once a week and titrated to maintain a serum level of 125 to 225 ng/ml. Methylprednisolone 250 mg IM was administered the morning of intramyocardial injection (14 days after MI) and tapered to 125 mg PO daily over the first 2 weeks after transplantation, then continued for the duration of the study.

Safety Endpoints

This preclinical study assessed a number of specified safety endpoints, including survival, body weight, and laboratory values (hematology, chemistry, and markers of cardiac injury, such as creatine phosphokinase); at study's end, hearts were harvested for analysis. The left ventricle was photographed and sliced into 10 4 mm thick rings along the short-axis plane.

Samples of infarcted myocardium, border zone, and noninfarcted heart were obtained and stored in formalin for analysis of histology. At necropsy, gross and microscopic tissue analysis was performed using samples from liver, spleen, kidney, lung and ileum tissue to look for the presence of neoplastic tissue (at necropsy) and histopathology analysis using Hematoxylin and Eosin or Masson's trichrome staining.

Analyses Performed

Heart sections were deparaffinized, rehydrated and antigen retrieved in 1 mmol/l citrate (pH 6.0) and nonspecific staining was blocked using 10% normal donkey serum for 1 hour at room temperature. Primary antibodies were incubated overnight at 4° C. Slides were washed in phosphate-buffered saline followed by secondary antibody incubation for 45 minutes at room temperature. Primary antibodies used: human mitochondria (1:600; Abcam, Cambridge, Massachusetts); phospho-histone H3 (pH3) (1:1500; Abcam); PIM-1 (1:30; Santa Cruz Biotechnology, Dallas, Texas; 1:30; Abcam), ckit (1:30; Sigma-Aldrich Co. LLC, St. Louis, Missouri), myosin light chain (1:100; Novus Biologicals, Littleton, Colorado), smooth muscle actin (sm22a) (1:1000, Abcam), endothelial cell (cd31) (1:1000, Abcam). The stained samples were first studied with immunofluorescent microscopy (Olympus LX81) and then a Zeiss LSM710 confocal microscope (Zeiss Corp, Oberkochen, Germany) to prepare images. Three to 4 slides were analyzed for each of the animals at 8 weeks post-injection for pH3 and human mitochondria. For myocyte cross-sectional area, sections were stained for membranes with fluorescein isothiocyanate-conjugated wheat germ agglutinin and measurements were performed using the National Institutes of Health public domain image-processing tool known as ImageJ.

CMR imaging was performed using a 3.0-T Magnetom clinical scanner (Siemens AG, Munich, Germany). All swine underwent serial cardiac CMR to evaluate global and regional function, including baseline (pre-MI), 2 weeks post-MI, then 2, 4, and 8 weeks after transepicardial cell delivery. CMR was used to establish efficacy endpoints: end-diastolic volume (EDV); end-systolic volume (ESV); scar size; ejection fraction (EF); stroke volume (SV); viable tissue; eulerian circumferential strain; and diastolic strain rate. Hemodynamic endpoints assessed included measures of preload (end-diastolic pressure), afterload (blood pressure and arterial elastance), contractility (preload-recruitable stroke work, and dp/dt max), lusitropy (dp/dt min, end-diastolic pressure volume relationship, tau [isovolumetric relaxation]), and integrated cardiac function (cardiac output, heart rate, end-systolic pressure volume [PV] relationship, SV, and EF). There is a strong correlation between scar size measured by CMR and scar size measured according to gross pathology sections (9); therefore, for these studies, scar size was measured using CMR only. CMR has been well established as a central prognostic tool to accurately detect and quantify myocardial fibrosis (10). Our laboratory has validated this technique in past studies (8,9). Total delayed enhanced mass was calculated using short axis images where the contours of the left ventricular (LV) wall was drawn automatically by the software and manually corrected when deemed necessary and the delayed enhanced area in each slice was highlighted automatically by the software (Figure 1, Online Figure 1).

Swine had a series of LV PV analysis. A micromanometer and cardiac conductance catheter (Millar Inc., Houston, Texas) was inserted through the arterial vascular sheath into the left ventricle. LV PV loops were recorded at rest and during transient balloon occlusion of the inferior vena cava in order to record a set of PV loops during decreasing preload and hemodynamic endpoints measured.

Statistical Analysis

Data are presented as mean ± SEM. Statistical software SPSS Version 21.0 (IBM Corporation, Armonk, New York) was used to analyze all data points. For within and between group comparisons, 1- and 2-way analysis of variance (ANOVA) repeated measures were applied with Bonferroni or Tukey multiple comparison tests as appropriate; both of which calculate intraindividual differences. We included all the data in the repeated measures analysis. We included the 4-week data points from the 8-week branch endpoint in with the 4-week data points from the 4-week branch endpoint. A $p < 0.05$ was considered statistically significant.

Results

Twenty-nine female Yorkshire pigs were included in the study that was composed of 2 arms: 4 and 8 weeks post-cell injection. There were 6 placebo, 6 hCSC, and 5 Pim1+ hCSC pigs in the 4-week arm and 4 additional per group for the 8-week study (Figure 2). Baseline and post-MI conditions for all animals are shown in Table 1. Body weights were measured at baseline and at scheduled points and there were no differences between the cell-treated and placebo groups (Online Figure 2A). Serum hematology, chemistry, and cardiac enzymes were measured at numerous predetermined time points throughout this study. None of the groups exhibited evidence of clinically relevant laboratory abnormalities (data not shown).

There were no deaths following cell transplantation in the placebo or cell-treated groups. Three animals in the placebo group were euthanized following veterinary consultation because they reached humane endpoints.

Whole body (liver, spleen, kidney, lung, and ileum) necropsies were performed to assess ectopic tissue formation. There were no observable signs of tumorigenicity or ectopic tissue formation on whole body necropsy at either time point following study product administration. There was a cyst found in the kidney of an hCSC-treated animal that was deemed benign by the veterinarian and not associated with the treatment. All animals receiving direct surgical injections tolerated them well, and there were no deaths related to treatment administration.

Histology

Hearts were serially sectioned from the apex to the base in 4 mm slices. Tissue samples were collected from each slice to include the infarct, border, and remote zones for a total of 30 samples per heart. Histological examination was performed by an experienced pathologist (A.M.) blinded to animal treatment.

Transmural infarcts were observed in all hearts. Infarcts were characterized by densely collagenized scar tissue with mild-to-moderate cellularity, due mostly to fibroblasts, and mild-to-moderate vascularity. There were rare, very small foci of inflammation composed of lymphocytes and macrophages, with minor myocyte damage and necrosis. Many hearts exhibited a mild degree of pericardial fibrosis, attributable to the surgical procedure. Rarely, small foci of mature fat and calcification within the scar were also observed, consistent with known histology (11) of healed MI.

Teratomas or other neoplastic processes were not identified in any of the hearts. Overall, no major differences were evident between placebo, hCSC, and Pim1+ hCSC animals.

Treatment Effects

The Pim1+ hCSC group produced a ~3-fold decrease in scar mass at 4 (−25 ± 3.8% vs. −6.6 ± 3.3%; $p < 0.001$) and 8 weeks (−29.7 ± 2.7% vs. −8.4 ± 0.7%; $p < 0.001$) post-transplantation compared to hCSCs, while no significant changes were observed in scar in the placebo group (Table 1, Figure 1). Additionally, Pim1+ hCSC injections produced a 2-fold increase in viable mass compared to hCSCs at 8 weeks (113.7 ± 7.2% vs. 65.6 ± 6.8%; $p < 0.003$) (Table 1). Increase in viable myocardial mass was not due to hypertrophy as there were no significant differences in LV mass/body weight ratio (Online Figure 2B) and myocyte cross-sectional area in the 3 groups (Online Figure 3).

EDV and ESV volumes increased similarly in all 3 groups compared to baseline (Table 1). There was a greater increase in regional contractility at the infarct zone (−10 ± 1.1 vs. −6.1 ± 0.3, respectively; $p < 0.05$) and border zone (−12.3 ± 1 vs. −8.4 ± 0.5 respectively; $p < 0.05$) in the 2 cell groups whereas the placebo group continued to deteriorate (Figure 3). Stroke work increased in all groups; however, while both cell-treated groups exhibited a similar improvement compared to placebo at 4 weeks post-injection, the effect was sustained in the Pim1+ hCSCs for at least 4 more weeks compared to hCSCs (Figure 4A). Cardiac output showed a similar pattern (Figure 4B). As a result, LVEF improved in both cell-treated groups at 4 weeks compared to placebo (Pim1+ hCSC: 14.2 ± 1.2% vs. hCSC: 9.1 ± 1.9% vs. placebo: 0.9 ± 1.4; change from pre-injection, $p < 0.001$) but this improvement was sustained only in the Pim1+ hCSC group (Pim1+ hCSC: 12.7 ± 1.7% vs. hCSC: 5.1 ± 3.1% vs. placebo: −0.7 ± 2.5%, change from pre-injection, 2-way ANOVA $p < 0.001$) at 8 weeks (Figure 4C).

While stroke work increased in the Pim1+ hCSC group at 4 and 8 weeks post-delivery compared to placebo (Figure 4A), mechanical energy used (PV area) in both groups remained unchanged (data not shown). This combination resulted in improved mechanoenergetic recoupling in the Pim1+ hCSC group (cardiac efficiency: 46 ± 3% vs. 32 ± 1%; $p = 0.005$) (Figure 4D).

Preload recruitable stroke work, a load-independent measure of contractility, was increased significantly at 8 weeks in hCSC group as compared to pre-injection levels (from 34.3 ± 4.2 mm Hg to 46 ± 5.45 mm Hg; $p = 0.005$) but this increase was not seen in the Pim1+ hCSC group at 8 weeks (from 27.25 ± 4.5 mm Hg to 41.2 ± 11.42 mm Hg; $p = 0.36$) (Figure 5A). While end-systolic PV relationship, another measure of contractility, showed no change in

the Pim1+ hCSC group (1.4 ± 0.6 mm Hg/ml vs. pre-injection levels of 1.0 ± 0.2 mm Hg/ml; p = 0.66) or in the hCSC group compared to pre-injection levels (1.4 ± 0.1 mm Hg/ml vs. 1.3 ± 0.2 mm Hg/ml; p = 0.52) (Online Table 1).

Both hCSC and Pim1+ hCSC reduced afterload (arterial elastance: hCSC −28.2 ± 6.1%; p = 0.02; and Pim1+ hCSC −45.7 ± 5.9%; p = 0.004), compared to pre-injection levels but there was no significant difference between the 2 cell treatment groups (p = 0.08) (Figure 5B).

Engraftment and differentiation of injected cells was assessed 8 weeks after treatment by staining for human mitochondria. Hearts obtained from placebo-injected animals served as the negative control (Online Figure 4A), whereas the positive control consisted of an unmanipulated porcine heart that was fixed immediately following ex vivo Pim1+ hCSC injection (Online Figure 4B). Positive staining for human mitochondria was present in cardiomyocytes and noncardiomyocyte cells from Pim1+ hCSC-injected animals (7.57 ± 5.8 cells/cm^2) (Figures 6A and 6C, Online Figure 4C) and hCSC animals (0.94 ± 0.6 cells/cm^2) (Figure 6B), with significant differences present between Pim1+ hCSC-injected animals relative to the placebo group. Colocalization of ckit and Pim1 was observed in hCSC animals (Online Figure 5), with colocalization of human mitochondria and Pim1 in both hCSC animals (Figure 6B) as well as Pim1+ hCSC-injected animals (Figure 6A), suggesting persistent Pim1 expression at 8 weeks post-delivery of cells.

Mitotic cells were revealed by phospho-Histone3 (pH3) within the myocardium costained with markers for cardiomyocyte (myosin light chain), endothelial cell (CD31), and smooth muscle cell (sm22a) cell lineages and then analyzed using 11 to 12 slides per group. pH3+ cardiomyocytes were increased in the border zone in the Pim1+ hCSC-injected group compared to placebo. Significant differences were not observed when assessing pH3+ labeling of noncardiomyocyte cells (endothelial and smooth muscle) among the 3 groups (Figure 7, Online Figure 6).

Discussion

This preclinical, placebo-controlled, blinded study compared safety and efficacy of c-kit+ CSCs to genetically-modified CSCs that overexpress Pim1, a proto-oncogenic serine-threonine kinase (Pim1+ CSCs) in a porcine model of acute MI. Neither cell produced increased adverse effects compared to placebo. No ectopic tissue formation was detected, confirming previously published findings in a porcine (8) and murine model (2), respectively. Furthermore, this is the first demonstration that Pim1 overexpression potentiates antifibrotic and cardioreparative capabilities of hCSCs in a large animal model. Reduction in scar size and increased proportion of viable tissue was coupled to significant functional improvement as indicated by improved LV SV, EF, and contractility. Scar size, as measured by delayed gadolinium enhancement, was substantially reduced and replaced by viable myocardial tissue able to contract (improved contractility) suggestive of myocardial regeneration and repair. PV area, which is closely associated with chemical energy consumed by myocardium per contraction (12) remained unchanged in all 3 groups, but the amount of energy converted into mechanical energy (as measured by stroke work) was significantly larger in the Pim1+ hCSC group at 8 weeks post injection, leading to a higher

ratio of cardiac efficiency. Furthermore, Pim1+ hCSC at 8 weeks post-delivery showed increased pH3+ cardiomyocyte immunolabeling, and both cardiomyocytes and noncardiomyocytes demonstrated evidence of human mitochondria. Pim1+ hCSCs may differentiate into cardiomyocytes and/or transfer mitochondria to cardiomyocytes, but further study is needed to establish the basis for mitochondrial persistence.

CSCs are a resident cardiac stem cell population located within niches in the heart (13) that play important developmental (14), regulatory, and regenerative roles (15), although the mechanism of regeneration remains controversial (16,17). A consensus is emerging that CSCs participate in repair and can differentiate into cardiomyocytes (14). Preclinical studies (18) and clinical trials (19–21) demonstrated that CSCs have an excellent safety record and exhibit therapeutic efficacy (22,23). Greater improvement in both structural and functional parameters seen in the Pim1+ hCSC group has important clinical implications for the use of this next-generation stem cell therapy approach.

With current approaches, the vast majority of transplanted stem cells are lost due to apoptosis or poor retention post-delivery, potentially offsetting their long-term efficacy (1,24,25). The presence of human mitochondria within porcine cardiomyocytes 8 weeks following Pim1+ hCSC injection suggested that Pim1 overexpression enhances survival, differentiation, and/or other direct cell-cell effects of CSCs. Our group previously demonstrated that combining CSCs and mesenchymal stem cells produces a synergistic effect, leading to greater cardioreparative capabilities compared to that observed using each cell type alone (8,9). Here we demonstrated that hCSCs overexpressing Pim1 provided enhanced therapeutic benefit relative to control CSCs in a large animal model, confirming prior findings from a murine model of MI (2). The magnitude of this benefit may be dependent on the intracellular localization of Pim1 (26).

Several studies (27,28) proposed genetic modification to enhance reparative function, based on the rationale that ex vivo manipulation of stem cells leads to enhanced cellular survival, secretion of paracrine factors, and activation of endogenous repair mechanisms (24). Among these studies, the Akt kinase, a pro-survival kinase, stands out as an attractive target but its effectiveness is limited by the fact that it does not directly participate in de novo tissue formation (29). Pim1 kinase is activated downstream of nuclear Akt signaling and possesses a compelling pro-survival/reduced senescence profile that includes stabilization of proliferative proteins through phosphorylation or direct association (30). Overexpression of Pim1 is associated with enhanced cell survival (3), elongation of telomeres (31), enhanced metabolic activity (32), attenuation of cell apoptosis (33), and preservation of mitochondrial integrity (34). In summary, Pim1+ hCSC proved to be superior therapy in a porcine model of MI, suggesting similar approaches will benefit patients.

Study Limitations

The continuous growth of the Yorkshire swine may obscure cardiac improvements, particularly volumetric measurements (EDV, ESV, and SV). However, all 3 groups exhibited a similar growth trend, thereby compensating for this limitation. The use of a xenogeneic graft (hCSCs) required the use of immunosuppression and may have affected the outcomes in all 3 groups, albeit equally. Although use of autologous or allogeneic swine cKit+ cells

could potentially overcome some immunologic challenges previously described (8), the large-animal xenogeneic model has the advantage of high translational relevance for future ex vivo manufacturing, engineering, and adoptive transfer capacity of human Pim1 CSCs as well as for acquiring clinically relevant experimental data enabling regulatory approval of genetically altered human CSCs. Green fluorescent protein (GFP) expression originating from CSCs was not observed in tissue sections, possibly because: 1) GFP is inherently difficult to detect in formalin-fixed, paraffin-embedded tissues (35–37): and/or 2) the CMV promoter used to engineer PIM1+ CSC is susceptible to epigenetic silencing in vivo, and particularly under hypoxic conditions (36,37). Finally, age of the donor might influence the donated stem cell's cardioreparative ability (38,39). Previous studies demonstrated Pim1's capacity to "rejuvenate" properties of aged stem cells (5); this could help account for the beneficial outcome using Pim1-modified CSCs considering that CSCs in the present study were obtained from a 65-year-old male in acute heart failure receiving an LV assist device. Allogeneic approaches (40) may offer an alternative that would derive CSCs from younger healthy donor populations.

Conclusions

At 8 weeks post-transplantation, transepicardial injection of human c-kit+ hCSCs genetically modified to overexpress Pim1 kinase reduced scar size, increased viable tissue, and restored contractile function toward normal. This approach provides a rationale for further exploration of the genetic modification of stem cells and consequent translation to clinical trials.

Supplementary Material

Refer to Web version on PubMed Central for supplementary material.

Acknowledgments

Sources of Funding: This study was supported by the National Institutes of Health (NIH) grant R01 HL084275 to JMH. JMH is also supported by NIH grants R01 HL107110, R01 HL110737 and 5UM HL113460. Dr. Karantalis was supported by a postdoctoral fellowship award from the American Heart Association. M.A. Sussman is supported by National Institutes of Health (NIH) grants: R01HL067245, R37HL091102, R01HL105759, R01HL113647, R01HL117163, P01HL085577, and R01HL122525, as well as an award from the Fondation Leducq.

We thank Jose Rodriguez, David Valdes and Marcos Rosado for expert technical assistance and Jose Da Silva for preparation of the cells.

Abbreviations And Acronyms

CMR	cardiac magnetic resonance
EDV	end-diastolic volume
EF	ejection fraction
ESV	end-systolic volume
hCSC	human cardiac stem cell

LV	left ventricular
MI	myocardial infarction

References

1. Golpanian S, Wolf A, Hatzistergos KE, Hare JM. Rebuilding the Damaged Heart: Mesenchymal Stem Cells, Cell-Based Therapy, and Engineered Heart Tissue. Physiol Rev. 2016; 96:1127–68. [PubMed: 27335447]
2. Fischer KM, Cottage CT, Wu W, et al. Enhancement of myocardial regeneration through genetic engineering of cardiac progenitor cells expressing Pim-1 kinase. Circulation. 2009; 120:2077–87. [PubMed: 19901187]
3. Muraski JA, Rota M, Misao Y, et al. Pim-1 regulates cardiomyocyte survival downstream of Akt. Nat Med. 2007; 13:1467–75. [PubMed: 18037896]
4. Mohsin S, Khan M, Toko H, et al. Human cardiac progenitor cells engineered with Pim-I kinase enhance myocardial repair. J Am Coll Cardiol. 2012; 60:1278–87. [PubMed: 22841153]
5. Fischer KM, Cottage CT, Konstandin MH, et al. Pim-1 kinase inhibits pathological injury by promoting cardioprotective signaling. J Mol Cell Cardiol. 2011; 51:554–8. [PubMed: 21255581]
6. Mohsin S, Khan M, Nguyen J, et al. Rejuvenation of human cardiac progenitor cells with Pim-1 kinase. Circ Res. 2013; 113:1169–79. [PubMed: 24044948]
7. McCall FC, Telukuntla KS, Karantalis V, et al. Myocardial infarction and intramyocardial injection models in swine. Nat Protoc. 2012; 7:1479–96. [PubMed: 22790084]
8. Williams AR, Hatzistergos KE, Addicott B, et al. Enhanced effect of combining human cardiac stem cells and bone marrow mesenchymal stem cells to reduce infarct size and to restore cardiac function after myocardial infarction. Circulation. 2013; 127:213–23. [PubMed: 23224061]
9. Karantalis V, Suncion-Loescher VY, Bagno L, et al. Synergistic Effects of Combined Cell Therapy for Chronic Ischemic Cardiomyopathy. J Am Coll Cardiol. 2015; 66:1990–9. [PubMed: 26516002]
10. Ambale-Venkatesh B, Lima JA. Cardiac MRI: a central prognostic tool in myocardial fibrosis. Nat Rev Cardiol. 2015; 12:18–29. [PubMed: 25348690]
11. Swindle MM, Makin A, Herron AJ, Clubb FJ Jr, Frazier KS. Swine as models in biomedical research and toxicology testing. Vet Pathol. 2012; 49:344–56. [PubMed: 21441112]
12. Nozawa T, Cheng CP, Noda T, Little WC. Effect of exercise on left ventricular mechanical efficiency in conscious dogs. Circulation. 1994; 90:3047–54. [PubMed: 7994853]
13. Beltrami AP, Barlucchi L, Torella D, et al. Adult cardiac stem cells are multipotent and support myocardial regeneration. Cell. 2003; 114:763–76. [PubMed: 14505575]
14. Hatzistergos KE, Takeuchi LM, Saur D, et al. cKit+ cardiac progenitors of neural crest origin. Proc Natl Acad Sci U S A. 2015; 112:13051–6. [PubMed: 26438843]
15. Urbanek K, Cesselli D, Rota M, et al. Stem cell niches in the adult mouse heart. Proc Natl Acad Sci U S A. 2006; 103:9226–31. [PubMed: 16754876]
16. van Berlo JH, Kanisicak O, Maillet M, et al. c-kit+ cells minimally contribute cardiomyocytes to the heart. Nature. 2014; 509:337–41. [PubMed: 24805242]
17. Ellison GM, Vicinanza C, Smith AJ, et al. Adult c-kit(pos) cardiac stem cells are necessary and sufficient for functional cardiac regeneration and repair. Cell. 2013; 154:827–42. [PubMed: 23953114]
18. Leri A, Kajstura J, Anversa P. Role of cardiac stem cells in cardiac pathophysiology: a paradigm shift in human myocardial biology. Circ Res. 2011; 109:941–61. [PubMed: 21960726]
19. Bolli R, Chugh AR, D'Amario D, et al. Cardiac stem cells in patients with ischaemic cardiomyopathy (SCIPIO): initial results of a randomised phase 1 trial. Lancet. 2011; 378:1847–57. [PubMed: 22088800]
20. Makkar RR, Smith RR, Cheng K, et al. Intracoronary cardiosphere-derived cells for heart regeneration after myocardial infarction (CADUCEUS): a prospective, randomised phase 1 trial. Lancet. 2012; 379:895–904. [PubMed: 22336189]

21. Yacoub MH, Terrovitis J. CADUCEUS, SCIPIO, ALCADIA: Cell therapy trials using cardiac-derived cells for patients with post myocardial infarction LV dysfunction, still evolving. Glob Cardiol Sci Pract. 2013; 2013:5–8. [PubMed: 24688997]
22. Karantalis V, Balkan W, Schulman IH, Hatzistergos KE, Hare JM. Cell-based therapy for prevention and reversal of myocardial remodeling. Am J Physiol Heart Circ Physiol. 2012; 303:H256–70. [PubMed: 22636682]
23. Telukuntla KS, Suncion VY, Schulman IH, Hare JM. The advancing field of cell-based therapy: insights and lessons from clinical trials. J Am Heart Assoc. 2013; 2:e000338. [PubMed: 24113326]
24. Terrovitis JV, Smith RR, Marban E. Assessment and optimization of cell engraftment after transplantation into the heart. Circ Res. 2010; 106:479–94. [PubMed: 20167944]
25. Keith MC, Tang XL, Tokita Y, et al. Safety of intracoronary infusion of 20 million C-kit positive human cardiac stem cells in pigs. PloS One. 2015; 10:e0124227. [PubMed: 25905721]
26. Samse K, Emathinger J, Hariharan N, et al. Functional Effect of Pim1 Depends upon Intracellular Localization in Human Cardiac Progenitor Cells. J Biol Chem. 2015; 290:13935–47. [PubMed: 25882843]
27. Dai Y, Xu M, Wang Y, Pasha Z, Li T, Ashraf M. HIF-1alpha induced-VEGF overexpression in bone marrow stem cells protects cardiomyocytes against ischemia. J Mol Cell Cardiol. 2007; 42:1036–44. [PubMed: 17498737]
28. Mangi AA, Noiseux N, Kong D, et al. Mesenchymal stem cells modified with Akt prevent remodeling and restore performance of infarcted hearts. Nat Med. 2003; 9:1195–201. [PubMed: 12910262]
29. Gnecchi M, He H, Noiseux N, et al. Evidence supporting paracrine hypothesis for Akt-modified mesenchymal stem cell-mediated cardiac protection and functional improvement. FASEB J. 2006; 20:661–9. [PubMed: 16581974]
30. Wang Z, Bhattacharya N, Weaver M, et al. Pim-1: a serine/threonine kinase with a role in cell survival, proliferation, differentiation and tumorigenesis. J Vet Sci. 2001; 2:167–79. [PubMed: 12441685]
31. Cottage CT, Neidig L, Sundararaman B, et al. Increased mitotic rate coincident with transient telomere lengthening resulting from pim-1 overexpression in cardiac progenitor cells. Stem cells. 2012; 30:2512–22. [PubMed: 22915504]
32. Borillo GA, Mason M, Quijada P, et al. Pim-1 kinase protects mitochondrial integrity in cardiomyocytes. Circ Res. 2010; 106:1265–74. [PubMed: 20203306]
33. Shirogane T, Fukada T, Muller JM, Shima DT, Hibi M, Hirano T. Synergistic roles for Pim-1 and c-Myc in STAT3-mediated cell cycle progression and antiapoptosis. Immunity. 1999; 11:709–19. [PubMed: 10626893]
34. Sussman MA. Mitochondrial integrity: preservation through Akt/Pim-1 kinase signaling in the cardiomyocyte. Expert Rev Cardiovasc Ther. 2009; 7:929–38. [PubMed: 19673671]
35. Hatzistergos KE, Quevedo H, Oskouei BN, et al. Bone marrow mesenchymal stem cells stimulate cardiac stem cell proliferation and differentiation. Circ Res. 2010; 107:913–22. [PubMed: 20671238]
36. Wendland K, Thielke M, Meisel A, Mergenthaler P. Intrinsic hypoxia sensitivity of the cytomegalovirus promoter. Cell Death Dis. 2015; 6:e1905. [PubMed: 26469954]
37. Walter I, Fleischmann M, Klein D, et al. Rapid and sensitive detection of enhanced green fluorescent protein expression in paraffin sections by confocal laser scanning microscopy. Histochem J. 2000; 32:99–103. [PubMed: 10816074]
38. Sousounis K, Baddour JA, Tsonis PA. Aging and regeneration in vertebrates. Curr Top Dev Biol. 2014; 108:217–46. [PubMed: 24512711]
39. Fan M, Chen W, Liu W, et al. The effect of age on the efficacy of human mesenchymal stem cell transplantation after a myocardial infarction. Rejuvenation Res. 2010; 13:429–38. [PubMed: 20583954]
40. Hare JM, Fishman JE, Gerstenblith G, et al. Comparison of allogeneic vs autologous bone marrow-derived mesenchymal stem cells delivered by transendocardial injection in patients with ischemic

cardiomyopathy: the POSEIDON randomized trial. JAMA. 2012; 308:2369–79. [PubMed: 23117550]

Perspectives

COMPETENCY IN MEDICAL KNOWLEDGE

In a porcine model of acute MI, genetically modified CSCs that overexpress Pim1, a proto-oncogenic serine-threonine kinase (Pim1+ CSCs), exhibited potentiated antifibrotic and cardioreparative properties.

TRANSLATIONAL OUTLOOK

Further studies are needed to explore potential therapeutic applications of Pim1 kinase activation in patients with acute MI.

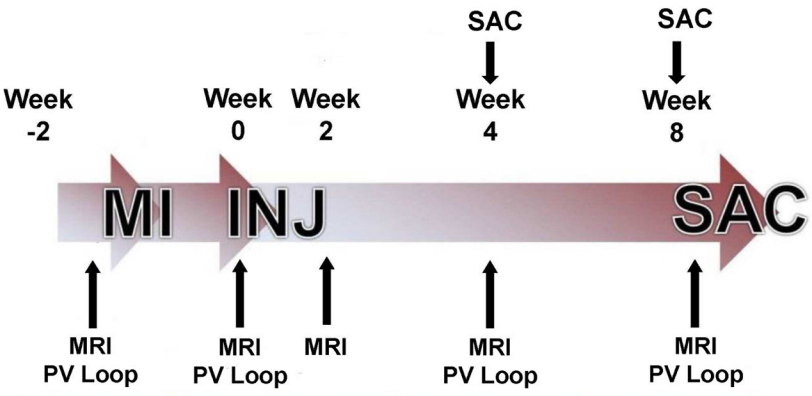

Placebo	10	10	10	7	4
hCSC	10	10	10	10	4
PIM1+ hCSC	9	9	9	9	4

Figure 1. Antifibrotic Effects

(**A**) At 4 and 8 weeks post-injection, both cell-treated groups exhibited decreased scar formation. In the PIM1^{+} human cardiac stem cell (hCSC) group, the antifibrotic effect was enhanced 3-fold compared to hCSC group. Representative examples of delayed enhancement of the myocardium using gadolinium cardiac magnetic resonance (CMR) images from placebo **(B)**, hCSC **(C)**, or Pim1^{+} hCSC **(D)** treated animals depict the progress of the delayed enhancement at the same location throughout different time points during the study. *$p < 0.05$ vs. pre-injection time; $^{\dagger}p < 0.05$ PIM1^{+} hCSC vs. hCSC and placebo; $^{\ddagger}p < 0.05$ PIM1^{+} hCSC vs. hCSC and placebo and hCSC vs. placebo.

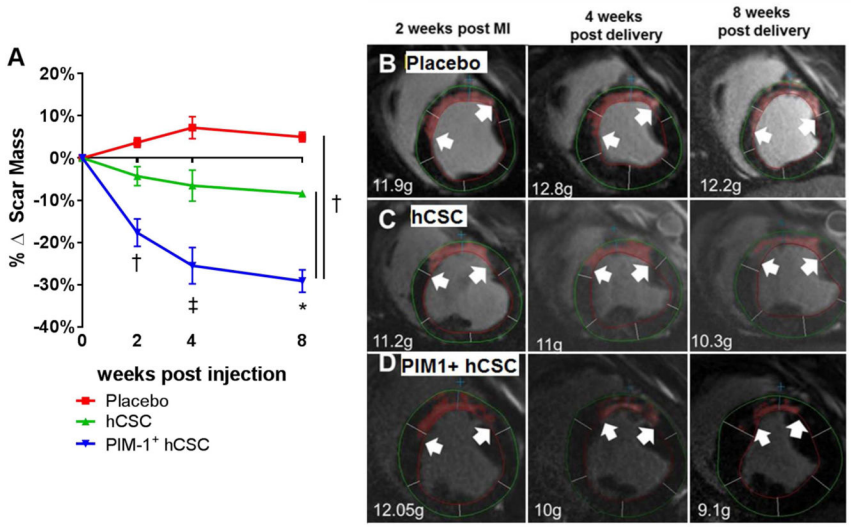

Figure 2. Study Timeline

The study was composed of 2 branches, with either a 4- or 8-week follow-up after injection (INJ). A series of CMR studies and pressure volume (PV) loop studies were conducted throughout the study as indicated. The table represents the number of animals per group at each time point. MI = myocardial infarction; SAC = sacrifice; other abbreviations as in Figure 1.

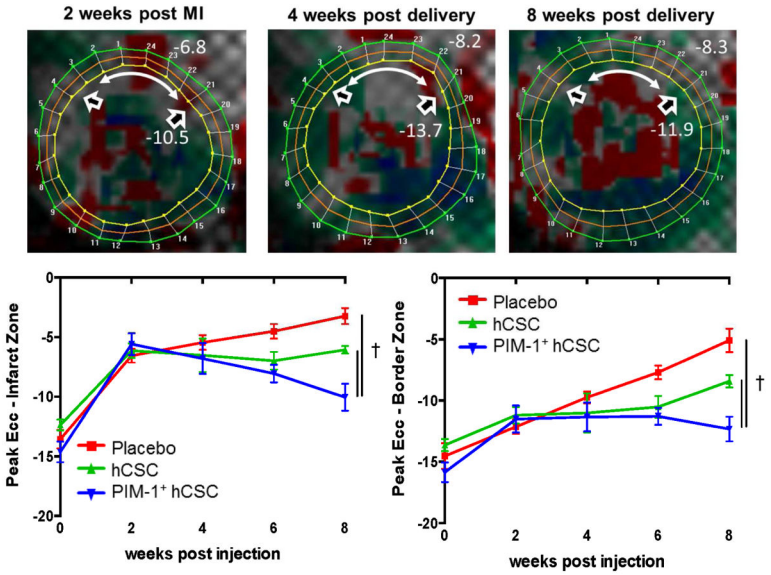

Figure 3. Improved Contractility Measured by Systolic Strain

(A) Eulerian circumferential strain (Ecc) is a measure of contractility; the more negative the value, the better the contractility. At 2 weeks post-MI (pre-injection) the contractility at the anteroseptal wall (in red) was greatly impaired (white double-headed arrow = infarct zone; open arrowheads = bordering zone). At 4 weeks post-delivery of $Pim1^+$ hCSCs, contractility started to improve (in gray) and at 8 weeks, areas at the infarct zone approached near normal contractility levels (in green). In both the infarct **(B)** and border **(C)** zones, the $Pim1^+$ hCSC group demonstrated greater improvement in contractility at 8 weeks than the other groups. $^{\dagger}p < 0.05$ $PIM1^+$ hCSC vs. hCSC and placebo. Abbreviations as in Figures 1 and 2.

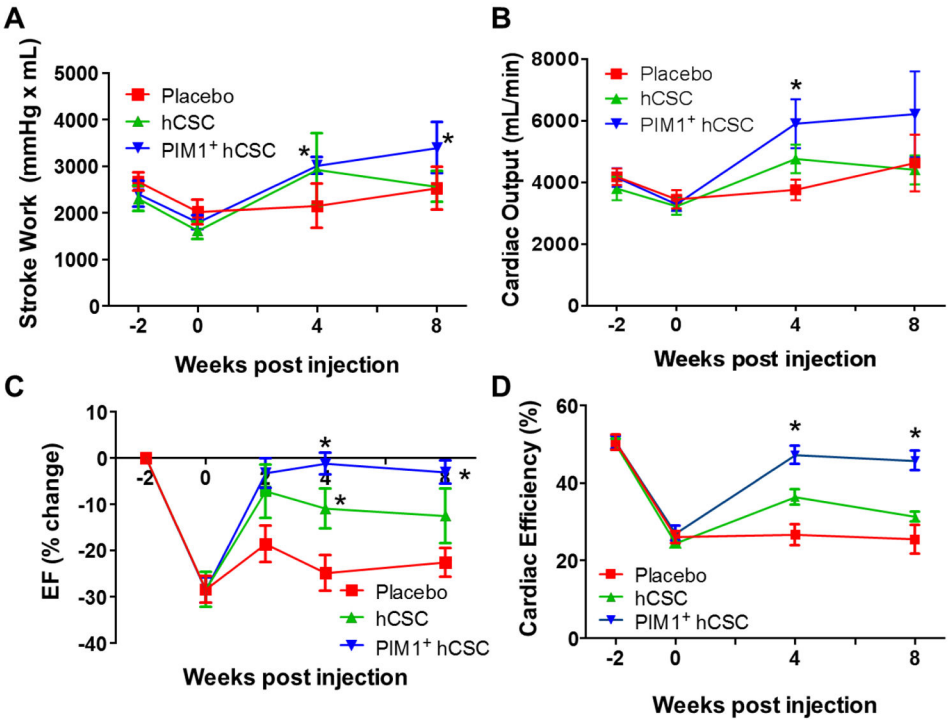

Figure 4. Cardiac Function

At 8 weeks post-injection, (**A**) stroke work and (**B**) cardiac output both improved in the Pim1^{+} hCSCs treated animals compared to pre-injection levels while the hCSC- and placebo-treated animals remained unchanged. (**C**) Left ventricular ejection fraction (EF) improved in both cell groups at 4 weeks compared to placebo, but this improvement was sustained only in the Pim1^{+} hCSCs group at 8 weeks. (**D**) Cardiac efficiency, the ratio of used mechanical energy to chemical energy consumed by the myocardium per beat, was restituted to near normal levels at 4 and at 8 weeks post-injection in the Pim1^{+} hCSC-treated animals while remaining unchanged in the placebo group. *$p < 0.05$ vs. pre-injection time. Abbreviations as in Figure 1.

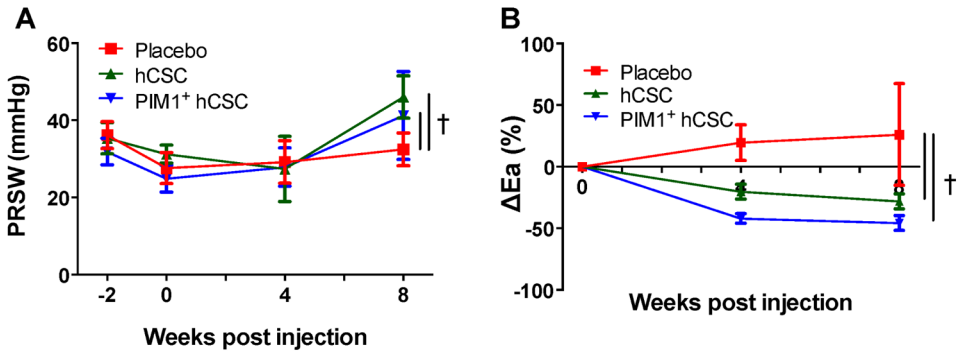

Figure 5. PRSW and Arterial Elastance

Injection of hCSCs improved (**A)** preload recruitable stroke work (PRSW) and **(B)** change in arterial elastance (Ea) versus placebo. $^{\dagger}p < 0.05$ $PIM1^{+}$ hCSC vs. hCSC and placebo. Abbreviations as in Figure 1.

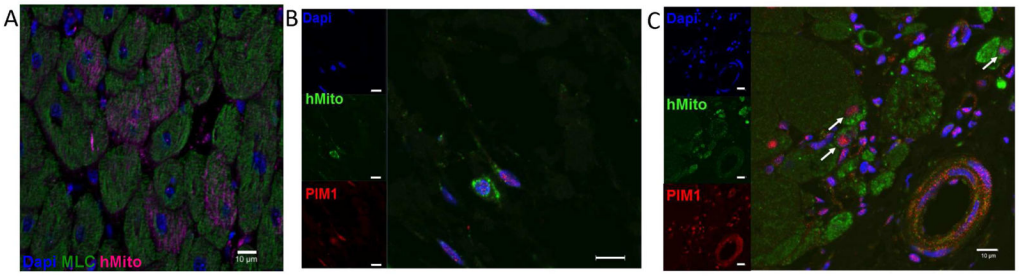

Figure 6. Pim1^{+} hCSCs Engraft and Differentiate

Localization of human mitochondrial marker is shown: **(A)** Confocal image depicts human mitochondria (red) costained with myosin light chain (green) and DAPI in Pim1^{+} hCSC animals 8 weeks after injection. Colocalization of human mitochondria (green), PIM1 (red), and nuclei (blue) is seen in hCSC animals **(B)** and PIM1+ hCSC-treated animals **(C)** at 8 weeks post-injection (arrows point to cells costained for both human mitochondria and PIM1). Scale bar = 10 μm. DAPI = 4’,6-diamidino-2- phenylindole; hMito = human mitochondria; other abbreviations as in Figure 1.

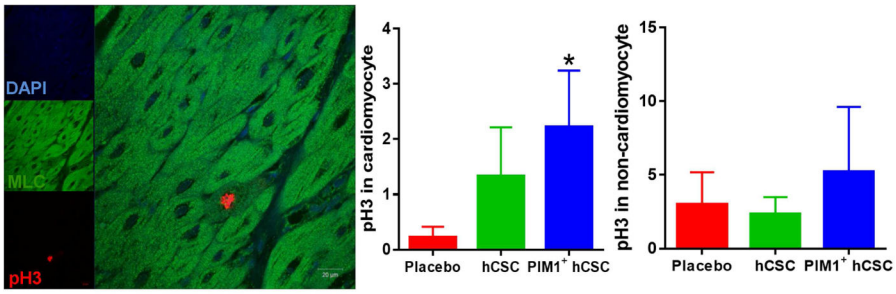

Figure 7. Mitotic Activity in Cardiomyocytes

(A) Confocal image depicts proliferating cells phospho-histone H3 (pH3) costained with myosin light chain (MLC) and DAPI. **(B)** Mitotic activity of endogenous cardiomyocytes (pH3) increased in the border zone in $Pim1^+$ hCSC-injected animals as compared to placebo 8 weeks post-injection ($p < 0.05$). **(C)** There were no significant differences in mitotic activity within noncardiomyocyte cells. Scale bar = 20 μm. *$p < 0.05$ $Pim1^+$ hCSCs vs. placebo. Abbreviations as in Figures 1 and 6.

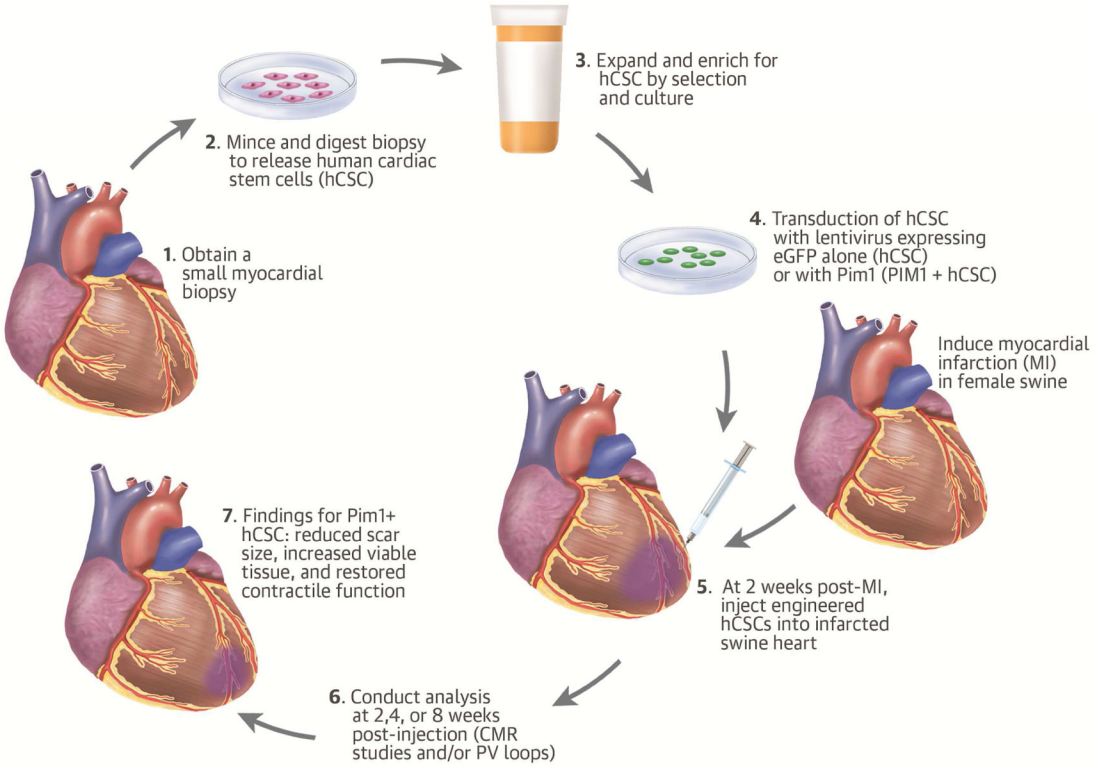

Central Illustration. Pim1 Overexpression Enhances Cardiac Repair

Following ischemia/reperfusion injury in swine, genetically engineered human cardiac stem cell (hCSC) with $Pim1^{+}$ reduced scar size, increased viable tissue, and restored contractile function towards normal 8 weeks post-injection. Cardiac magnetic resonance imaging and pressure volume (PV) loop analyses showed that $PIM1^{+}$ overexpression enhanced the cardioreparative capabilities of hCSCs. eGFP = enhanced green fluorescent protein.

J Am Coll Cardiol. Author manuscript; available in PMC 2017 December 06.

Table 1

Cardiac Magnetic Resonance Variables

Variable	Baseline Absolute Values	2 Weeks Post-MI (%Δ) or Absolute Value	4 Weeks Post-injection (%Δ)	p value	8 Weeks Post-injection (%Δ)	P value
EDV						
Placebo	88.8 ± 5.2ml	13.2 ± 7.3%	37.7 ± 7.9%	<0.05	42.96 ± 7.6%	<0.05
hCSC	79.9 ± 5.7ml	32.3 ± 9.4%	57.8 ± 16.8%	<0.05	76.7 ± 26.7%	<0.05
Pim1$^+$ hCSC	81.5 ± 4.8ml	29.5 ± 10.4%	53.3 ± 14.2%	<0.05	96.7 ± 23.1%	<0.05
ESV						
Placebo	41.1 ± 2.5ml	48.1 ± 11.3%	79.3 ± 15.3%	<0.05	84.01 ± 12.7%	<0.05
hCSC	40.8 ± 3.2ml	70.7 ± 15.9%	78.3 ± 25.7%	<0.05	103.9 ± 39.1%	<0.05
Pim1$^+$ hCSC	38.4 ± 2.1ml	71.9 ± 14.5%	58.6 ± 17.2%	<0.05	106.7 ± 27.1%	<0.05
SV						
Placebo	47.7 ± 3.4ml	−15.9 ± 6.3%	3.9 ± 6.01%	NS	10.6 ± 6.9%	NS
hCSC	39.1 ± 3ml	−7.16 ± 5.4%	37.7 ± 10.8%	<0.05	50.6 ± 14.8%	<0.05
Pim1$^+$ hCSC	43.1 ± 2.8ml	−9.1 ± 6.9%	47.9 ± 11.7%	<0.05	87.4 ± 18.9%	<0.05
Scar						
Placebo	N/A	12.8 ± 1.8g	6.98 ± 2.4%	NS	4.98 ± 1.2%	NS
hCSC	N/A	11.9 ± 1.1g	−6.6 ± 3.3%	NS	−8.4 ± 0.7%	<0.05
Pim1$^+$ hCSC	N/A	14 ± 1.4g	−25 ± 3.8%	<0.05	−29.2 ± 2.1%	<0.05
Scar/LVmass						
Placebo	N/A	15.4 ± 2.3%	−17.5 ± 3.6%	NS	−10.6 ± 8.7%	NS
hCSC	N/A	13.9 ± 0.9%	−25.1 ± 3.7%	<0.05	−40.6 ± 1.8%	<0.05
Pim1$^+$ hCSC	N/A	17.4 ± 2.1%	−41.2 ± 3.4%	<0.05	−62.5 ± 1.5%	<0.05
Viable Tissue						
Placebo	N/A	74.2 ± 4.2g	35.2 ± 6.5%	<0.05	42.2 ± 7.6%	<0.05
hCSC	N/A	73.1 ± 3.4g	33.7 ± 7%	<0.05	65.6 ± 6.8%	<0.05
Pim1$^+$ hCSC	N/A	68.1 ± 3.4g	43.7 ± 7.5%	<0.05	113.7 ± 7.2%	<0.05

Values are mean ± SEM.

All p values are derived from 1-way analysis of variance repeated measures. EDV = end-diastolic volume; ESV = end-systolic volume; hCSC = human cardiac stem cell; LV = left ventricular; MI = myocardial infarction; SV = stroke volume.